

March 7, 2023
**SELLA - A Program for Determining Bravais Lattice
Types**

LAWRENCE C. ANDREWS,^{a*} HERBERT J. BERNSTEIN^b AND NICHOLAS K. SAUTER^c

*^aRonin Institute, 9515 NE 137th St, Kirkland, WA, 98034-1820 USA, ^bRonin
Institute, c/o NSLS-II, Brookhaven National Laboratory, Upton, NY, 11973 USA,
Rochester Institute of Technology, c/o NSLS-II, Brookhaven National Laboratory,
Upton, NY, 11973 USA, and ^cLawrence Berkeley National Laboratory, 1 Cyclotron
Rd., Berkeley, CA, 94720 USA. E-mail: lawrence.andrews@ronininstitute.org*

Unit cell reduction; Delaunay; Delone; Niggli; Selling; Bravais Lattice

Abstract

We introduce a new Bravais lattice determination algorithm. SELLA is a straightforward algorithm and a program for determining Bravais lattice type based on Selling (Delone) reduction. It is a complete, closed solution, and it provides a clear metric of fit to each type.

Note: Boris Delaunay in his later publications used the Russian version of his surname: Delone. We will follow that choice.

1. Introduction

We introduce a new Bravais lattice determination algorithm. The Bravais lattice types were created by Bravais (1850). Delaunay (1932) and Niggli (1928) developed methods

for the identification of the Bravais lattice type of a crystal using the measured unit cell dimensions; their methods were exact only if the cell parameters exactly corresponded to the actual type (Patterson & Love, 1957). Delone discussed the issues of scalars that have nearly zero values, but the broader issues of other measurement errors were not discussed. Andrews & Bernstein (2014) review the literature on the efforts to create methods to utilize data that contain unavoidable measurement error.

SELLA is a algorithm and program for determining Bravais lattice type based on Selling (Delone) reduction. It is a complete, closed solution, and it provides a clear metric of fit to each type.

2. Terminology

Delaunay (1932) found that the 14 Bravais lattice types could be allocated among 24 types that are determined by the type of Dirichlet unit cell (termed the Voronoi region (Voronoi, 1908) or Dirichlet region (Dirichlet, 1850) by Delone). Delone used the convention of Bravais (1850) with the sides of the tetrahedron labeled by the labels of the six Selling scalars. Figure 1 shows the labeling used in the International Tables for Crystallography (Henry & Lonsdale, 1952); Table 1 shows other choices that have been used. The contents for each type are described in Figure 2.

CHARACTER

Burzlaff & Zimmermann (1985) revised the labeling of the types. Here we have returned to the numbering of the types to that of Delaunay (1932). In some cases, Delone included two forms within a single type. Burzlaff & Zimmermann (1985) renumbered by ordinals. Here we have labeled the Delone types that have multiple items as “A” and “B”. Table 2 shows the various labelings. Figure 3 recapitulates the figure of Delaunay (1932) using more modern notation. Table 1 lists the various labelings that have been used for the sides of the Bravais tetrahedron. Figure 1 shows the

arrangement of the symbols as used in the International Tables for Crystallography.

<i>(Delaunay, 1932)</i>	<i>(Burzlaff et al., 1992)</i>	<i>(Henry & Lonsdale, 1952)</i>	<i>(Patterson & Love, 1957)</i>	<i>(Andrews et al., 2019b)</i>
g	p	P	h ₂₃	s ₁
h	q	Q	h ₁₃	s ₂
k	r	R	h ₁₂	s ₃
l	s	S	h ₁₄	s ₄
m	t	T	h ₂₄	s ₅
n	u	U	h ₃₄	s ₆

Table 1. *The various terms used to describe the sides of the Bravais tetrahedron. (In the figures in Delaunay (1932) the tetrahedron has been rotated by -120 degrees)*

<i>(Delaunay, 1932)</i>	<i>(Burzlaff & Zimmermann, 1985)</i>	<i>this paper</i>
K _I	K1	C1
K _{III}	K2	C3
K _V	K3	C5
Q _I	Q1	T1
Q _{II}	Q2	T2
Q _V	Q3	T5
R _I	R1	R1
R _{III}	R2	R3
O _I	O1	O1A
O _I	O2	O1B
O _{II}	O3	O2
O _{III}	O4	O3
O _{IV}	O5	O4
O _V	O6	O5
M _I	M1	M1A
M _I	M2	M1B
M _{II} ₂	M3	M2A
M _{II}	M4	M2B
M _{III}	M5	M3
M _{IV}	M6	M4
T _I	T1	A1
T _{II}	T2	A2
T _{III}	T3	A3
H _{IV}	H1	H4

Table 2. *The 24 Delone types as labeled by various authors.*

2.1. The space \mathbf{S}^6

Andrews *et al.* (2019b) recast the Selling parameters to define a metric space,. We use the base vectors, \mathbf{a} , \mathbf{b} , \mathbf{c} of the unit cell to define $\mathbf{d} = -(\mathbf{a} + \mathbf{b} + \mathbf{c})$. A point s in \mathbf{S}^6 is defined as:

$$s = [s_1, s_2, s_3, s_4, s_5, s_6]$$

where $s_1 = \mathbf{b} \cdot \mathbf{c}$, $s_2 = \mathbf{a} \cdot \mathbf{c}$, $s_3 = \mathbf{a} \cdot \mathbf{b}$, $s_4 = \mathbf{a} \cdot \mathbf{d}$, $s_5 = \mathbf{b} \cdot \mathbf{d}$, and $s_6 = \mathbf{c} \cdot \mathbf{d}$.

2.2. Terminology of the Bravais lattice types

The Bravais tetrahedron symbol is used to display the relationships among the \mathbf{S}^6 scalars; see Figure 1 and Table 2 for descriptions. The different ways that the scalars have been labeled is in Figure 2. Figure 3 describes the information displayed for each Delone type.

3. Algorithms for creation of an exhaustive list of the polytopes of the Bravais types

3.1. Deriving the projectors and perps

We will use Selling reduction; Niggli reduction has a fundamental unit that is non-convex, and some boundaries of the fundamental unit are partly closed and partly open (Andrews & Bernstein, 2014) leading to considerable complexity. Because Niggli reduction divides the fundamental unit into separate all obtuse and all acute regions, the transitions between those are quite complex (Andrews & Bernstein, 2014). In space \mathbf{S}^6 (Andrews *et al.*, 2019a), the fundamental unit is the simple all-negative orthant of a 6-dimensional Cartesian space. Only two kinds of operations in the space will need to be considered: the 6 boundary transform operations at the boundaries of the orthant (zeros of an axis), and 24 reflections (Andrews *et al.*, 2019b)

Twenty-four lattice types were enumerated by Delaunay (1932). Three of those are triclinic, and we will ignore them because all crystals can be indexed as triclinic. We

shall need all representations of all non-triclinic lattice types within the \mathbf{S}^6 fundamental unit (all Selling-reduced cells) or those generated beyond the boundaries by boundary transforms. Three forms (M3, M2B, and O3) are reduced dimension boundaries that do not correspond to unique Bravais types; any lattice that falls in those three is indexed by one of the other 2 types or both. There remain 21, fully-6-dimensional, non-triclinic Delone lattice types.

Seven of the 21 Delone types do not have a zero in their \mathbf{S}^6 representation; the presence of zero indicates that a form is on the boundary of the \mathbf{S}^6 fundamental unit. Since a point on the boundary transforms to another boundary point (Andrews *et al.*, 2019a), we can generate the Virtual Cartesian Point (VCP) (Andrews *et al.*, 2019a) appropriate to each zero in the \mathbf{S}^6 vector. Because the reduction operations do not commute, in the cases where there is more than one zero in the vector, all orderings of applying reductions to all of the zeros must be generated. (For example, for two zeros, there will be six vectors produced.) Again, there may be many duplicate results.

Finally, the projectors must be computed for each of the many sample vectors of the 21 types. We will also need the “perps”, the operators that give the normal vector to each such manifold. For a particular polytope, the projector applied to the probe gives the least-squares best fit point within that polytope. Perps are computed by subtracting the corresponding projector from the unit matrix. The norm of a perp times a probe is the distance from that polytope.

3.1.1. Generating sample vectors from all Bravais types Step 1: Generate any random vector that contains no zero values and no duplicate values. For a later operation, it should only contain values large enough that adding or subtracting the smallest representable floating point number will not change the value in computer arithmetic (*DBL_MIN* in the C language).

Step 2: For each Delone type, multiply its projector by the vector from Step 1. Store the results in a list with entries for each type (see Table 5 for the projectors).

Step 3: a) If the vector contains no zeros, generate the 24 reflections and store in the list by type.

Step 3: b) If the vector contains one zero, apply the boundary transform operation for that boundary to the vector, and store the products of the vector and its 24 reflections in the list. Note, this is where the choice of *DBL_MIN* has effect; adding or subtracting such a small value will not change any value but zero. As a result, non-zero, integer values stored in floating point numbers will be unchanged.

Step 3: c) If the vector contains more than one zero and not *DBL_MIN*, first set the zero to *DBL_MIN*, and then return it to step b). Then set the second zero to *DBL_MIN* (with the first zero still zero), and send that result to step b). If there is a third zero, process it the same way as two zeros and return to c).

Continue to iterate those steps until all the types have been processed. There will be duplicates within each type, which will be eliminated later.

3.1.2. Generate projectors from sample vectors Each vector in the list from the previous steps is a representative of one of the Delone types. Although a vector is a one-dimensional polytope, these vectors encode the information about the full polytopes of the Delone types in their zeros and their duplicate values.

We begin by defining a function: Fraction that computes the reciprocal of the number of elements in the vector that equal an input value or zero if there are no duplicates.

The following steps will be repeated for each of the vectors in the list generated above. We generate a matrix m .

Step 1: Zero any scalars that have been set to *DBL_MIN*. The result will be that all permutations will be created.

Step 2: For each of the six scalars

For i in 1-6 $m[i,i] = \{\text{if } \textit{Fraction}(s[i]) == 0.0 \text{ or } \text{abs}(s[i]) == 0.0\} \text{ then } 0.0 \text{ else } \textit{Fraction}(s[i])$

For i in 1-6 For j in 1-6 $m[i,j] = \{\text{if } s[i]==s[j] \text{ or } \text{abs}(s[j]) > 0\} \text{ then } \textit{Fraction}(s[j])$
else 0.0

Add m to a list of the projectors.

To finish, the duplicate projectors are removed within each type, leaving 239 non-triclinic projectors. (If the triclinic cases are included, there are 10 more.) See Table 4.

3.2. Performing the fit

The distance from the given polytope is just the norm of the perp for that polytope applied to the probe.

4. Degenerate Delone types

Three of the 21 non-triclinic Delone types are only boundaries of other types. In Figure 4, Delone types M2B and M3 are in the row for orthorhombic, and O3 is in the row for rhombohedral and tetragonal. These types do not need to be searched for in general surveys.

5. Verification

5.1. Rationale

Most of the proposals for Bravais lattice determination in the presence of experimental error do not have a clear proof that they are complete. For many years there were verbal complaints that available programs would not infrequently miss experimental cases (for example, TRACER (Lawton & Jacobson, 1965) and many anecdotal

communications). To our knowledge, only the method of (Oishi-Tomiyasu, 2012) has clearly demonstrated completeness. The justification that Sella is complete has three parts.

First: We require that the cell being tested be reduced, and all Bravais lattice types within the \mathbf{S}^6 fundamental unit (all \mathbf{S}^6 scalars negative) be generated. Therefore, the 24 possible forms of a reduced cell will be close to one of the 24 copies of the types. For the reflections, we do not need to consider the case of points near a boundary that might be outside; the boundary transforms must be treated for that.

Second: In the case of the boundary transform operations, we take the case of a point that is infinitesimally distant from the polytope of a Bravais lattice type that has one zero in its scalars. Take the point in the polytope that is closest to the experimental point. We transform both by the corresponding boundary transform operation. We have generated a new pair of points in a different location, one of which is in some representation of the same Bravais lattice type. The generated points are still infinitesimally distant from each other.

Third: Assume we have a point that is outside the fundamental unit and is near an undiscovered polytope for a Bravais lattice type. If the point is near a boundary defined by a single zero, then we apply a boundary transform to the point and to the Bravais polytope, bringing them both into the fundamental unit. If all of the variations of all of the Bravais lattice types within and on the fundamental unit have been generated, then this putative undiscovered polytope has already been included in the list of possibilities. Similar arguments apply to the cases of two or three zeros.

If we apply all of the boundary transform operations to the representations of the Bravais lattice types, then there are no places that a point in the fundamental unit will fail to find the closest Bravais lattice (or lattices). As stated above, there are 239 non-triclinic possible representations.

What might occur if some reduced point has an unreduced copy near the all-negative orthant? Would it be possible for it to be close to one of the copies of one of the 21 Delone types? The corresponding reduced point is obviously in the all-negative orthant. Further, because all possible copies of all of the Delone type manifolds have been generated, the reduced point will be near a copy of the manifold it was near when it was unreduced.

5.2. Testing against known cells

89539 unit cells were extracted (April, 2019) from the Protein Data Bank (Bernstein *et al.* (1977) and Berman *et al.* (2000)). When evaluated with Sella, all but 57 were found at zero distance from the described crystal class. The 57 were identified as incorrect unit cells for the assigned crystal class; however, the distances from the assigned classes were small because the deviations from the appropriate parameters were modest (see Table 3).

PDB ID	Sp.Gr.	Delone type	distance (Å)	PDB ID	Sp.Gr.	Delone type	distance (Å)
1NUI	P3121	H4	0.0439	1SHN	P43212	T5	0.0491
1NUI	P3121	H4	0.0439	1C50	P43212	T5	1.9040
2NW8	P3121	H4	0.0401	2A1L	P43212	T5	0.0528
2J1L	P3121	H4	0.0307	1S2L	P43212	T5	0.0334
1VYI	P3121	H4	0.2504	1H9S	P41	T5	1.0149
3FZ8	P32	H4	0.0575	1H9R	P41	T5	1.0141
2J5W	P3221	H4	0.0543	2F0Q	P41	T5	0.0260
2VAM	P3221	H4	0.1166	3EYM	P41	T5	0.0476
1Y8J	P3221	H4	0.0389	1WV5	P41212	T5	0.0250
1F4V	P3221	H4	0.0276	2DF3	P41212	T5	0.0387
2ZP9	P6	H4	0.0528	1L6O	P41212	T5	0.0346
1DDR	P61	H4	0.0726	3A58	P41212	T5	0.2976
1DDS	P61	H4	0.0726	2IU9	P41212	T5	0.0373
1SGU	P61	H4	0.0295	4BTP	P41212	T5	0.0666
3CDC	P61	H4	0.0559	1W54	P4212	T5	0.0420
2WAG	P6122	H4	0.0377	2PBE	P42212	T5	0.0548
1LBM	P6122	H4	0.0312	3BR5	P42212	T5	0.2203
2O9Z	P62	H4	0.0402	1GMD	P42212	T5	0.1400
1ELZ	P6322	H4	0.4035	1GMC	P42212	T5	0.1402
1SA0	P65	H4	0.0681	2CCN	P42212	T5	0.0447
3KQI	P6522	H4	0.0331	1CE1	P212121	O5	0.6472
2F9Y	P6522	H4	0.0470	3DQ2	P212121	O5	0.1058
3E73	P6522	H4	0.0523	1Z2A	P212121	O5	0.0670
3CAP	H3	H4	0.0586	2HA3	P212121	O5	0.3070
2UX6	H32	H4	0.0386	3BNJ	I4122	T2	0.9518
1ODT	H32	H4	0.0816	4MGP	I-42d	T1	0.2128
2FDI	P43	T5	0.0758	4ASL	C2221	O4	0.3383
3HQ7	P43212	T5	0.2869	3K7M	P432	C5	0.0517
1E2Q	P43212	T5	0.5482	3GBN	I213	C1	1.2661

Table 3. Among the unit cell parameters extracted from the PDB, these 57 has cell parameters that did not conform to the assigned crystal types. In all cases, the differences were modest to small.

5.3. Testing for continuity

The polytopes of the Bravais lattice types are characterized by required zeros of scalars and/or multiplets of equal values. For instance, all primitive monoclinic cells have two 90 degree angles and so two zero scalars. Consider R1 as an example for multiplets. The character for R1 is (**rrrsss**); two triplets.

For the case of M4, primitive monoclinic, the character is (**00rstu**). For a particular value for r,s,t,u, the best monoclinic cell will not depend on whatever values are substituted for the zeros. In the plane corresponding to the two zero scalars, we can

draw a circle, each point on the circle corresponding to a lattice. Reducing each so perturbed lattice and calculating the distance of the reduced cell from (**00rstu**) will give a curve that should not have any discontinuities. See Figure 5.

Similarly, Bravais type O5 has a triplet of zeros, character (**000rst**). Here we can generate a sphere that surrounds the orthorhombic point. See Figure 6.

Bravais type O4 has two zeros and a pair of required equal values, character (**00rsst**). The zeros can be treated the same as above. The pair of equal values must have an average value that remains equal to **s** in the lattice character. That leaves 3 values to vary, and we can create a sphere around the point (**00rsst**). See Figure 7.

6. Comparisons

Comparison to other distance measure; Data for other measures taken from Andrews & Bernstein (2014).

Lattice character	G6 distance	BGAOL Z score	XDS QI	Scaled QI	Sella
mP	20.138	0.657	1.0	0.13	1.06
oC	125.958	3.560	23.	8 3.09	13.82
mC	125.150	4.085	23.	4 3.03	13.80

Acknowledgements Careful copy-editing and corrections by Frances C. Bernstein are gratefully acknowledged. Our thanks to Jean Jakoncic and Alexei Soares for helpful conversations and access to data and facilities at Brookhaven National Laboratory.

Funding information

Funding for this research was provided in part by: US Department of Energy Offices of Biological and Environmental Research and of Basic Energy Sciences (grant No. DE-AC02-98CH10886 ; grant No. E-SC0012704); U.S. National Institutes of Health (grant No. P41RR012408; grant No. P41GM103473; grant No. P41GM111244; grant No. R01GM117126, grant No. 1R21GM129570; grant No. P30GM133893); Dectris,

Ltd.

References

- Andrews, L. C. & Bernstein, H. J. (2014). *J. Appl. Cryst.* **47**(1), 346 – 359.
- Andrews, L. C., Bernstein, H. J. & Sauter, N. K. (2019a). *Acta Cryst.* **A75**.
<https://doi.org/10.1107/S2053273318015413>.
- Andrews, L. C., Bernstein, H. J. & Sauter, N. K. (2019b). *Acta Cryst.* **A75**, 115 – 120.
- Berman, H. M., Westbrook, J., Feng, Z., Gilliland, G., Bhat, T. N., Weissig, H., Shindyalov, I. N. & Bourne, P. E. (2000). *Nucleic Acids Res.* **28**, 235 – 242.
- Bernstein, F. C., Koetzle, T. F., Williams, G. J. B., Meyer, Jr., E. F., Brice, M. D., Rodgers, J. R., Kennard, O., Shimanouchi, T. & Tasumi, M. (1977). *J. Mol. Biol.* **112**, 535 – 542.
- Bravais, A. (1850). *J. Ecole. Polytech.* pp. 1 – 128.
- Burzlaff, H. & Zimmermann, H. (1985). *Z. Krist.-Crystalline Materials*, **170**(1-4), 247–262.
- Burzlaff, H., Zimmermann, H. & de Wolff, P. M. (1992). *International Tables for Crystallography, Vol. A*, chap. 9. Crystal Lattices, pp. 734 – 744. Dordrecht: Kluwer Academic Publishers.
- Delaunay, B. N. (1932). *Z. Krist.* **84**, 109 – 149.
- Dirichlet, G. L. (1850). *J. reine angew. Math.* **40**, 209.
- Henry, N. F. M. & Lonsdale, K. (eds.) (1952). *International tables for X-ray Crystallography*, vol. I, Symmetry Groups, chap. 5.1 Reduction of General Primitive Reciprocal-lattice Triplet to the Corresponding Conventional Bravais-lattice Triplet, pp. 530 – 535. Kynoch Press.
- Lawton, S. L. & Jacobson, R. A. (1965). *The reduced cell and its crystallographic applications*. Tech. rep. .
- Niggli, P., (1928). *Krystallographische und Strukturtheoretische Grundbegriffe*, Handbuch der Experimentalphysik, Vol. 7, part 1. Akademische Verlagsgesellschaft, Leipzig.
- Oishi-Tomiyasu, R. (2012). *Acta Cryst.* **A68**(5), 525 – 535.
- Patterson, A. L. & Love, W. E. (1957). *Acta Cryst.* **10**(2), 111–116.
- Voronoi, G. (1908). *Journal für die reine und angewandte Mathematik*, **133**, 97–178.
[Http://eudml.org/doc/149276](http://eudml.org/doc/149276).

Table 4. *The 21 non-triclinic Delone types with the count of representations. The asterisks indicate non-crystallographic types.*

Delone type	Count
H4	12
C1	1
C3	3
C5	16
R1	4
R3	12
T1	3
T2	6
T5	48
O1A	3
O1B	1
O2	6
O3*	9
O4	36
O5	16
M1A	6
M1B	3
M2A	12
M2B*	12
M3*	18
M4	12

Table 5. Projectors for the 24 Delone types

C1	(cI)	[1 1 1 1 1 1/ 1 1 1 1 1 1/ 1 1 1 1 1 1/ 1 1 1 1 1 1/ 1 1 1 1 1 1/ 1 1 1 1 1 1]
C3	(cF)	[1 1 0 1 1 0/ 1 1 0 1 1 0/ 0 0 0 0 0 0/ 1 1 0 1 1 0/ 1 1 0 1 1 0/ 0 0 0 0 0 0]
C5	(cP)	[0 0 0 0 0 0/ 0 0 0 0 0 0/ 0 0 0 0 0 0/ 0 0 0 1 1 1/ 0 0 0 1 1 1/ 0 0 0 1 1 1]
T1	(tI)	[1 1 0 1 1 0/ 1 1 0 1 1 0/ 0 0 1 0 0 1/ 1 1 0 1 1 0/ 1 1 0 1 1 0/ 0 0 1 0 0 1]
T2	(tI)	[1 1 0 1 1 0/ 1 1 0 1 1 0/ 0 0 0 0 0 0/ 1 1 0 1 1 0/ 1 1 0 1 1 0/ 0 0 0 0 0 1]
T5	(tP)	[0 0 0 0 0 0/ 0 0 0 0 0 0/ 0 0 0 0 0 0/ 0 0 0 1 1 0/ 0 0 0 1 1 0/ 0 0 0 0 0 1]
R1	(rP)	[1 1 1 0 0 0/ 1 1 1 0 0 0/ 1 1 1 0 0 0/ 0 0 0 1 1 1/ 0 0 0 1 1 1/ 0 0 0 1 1 1]
R3	(rP)	[1 1 0 0 1 0/ 1 1 0 0 1 0/ 0 0 0 0 0 0/ 0 0 0 1 0 0/ 1 1 0 0 1 0/ 0 0 0 0 0 0]
O1A	(oF)	[1 1 0 1 1 0/ 1 1 0 1 1 0/ 0 0 1 0 0 0/ 1 1 0 1 1 0/ 1 1 0 1 1 0/ 0 0 0 0 0 1]
O1B	(oI)	[1 0 0 1 0 0/ 0 1 0 0 1 0/ 0 0 1 0 0 1/ 1 0 0 1 0 0/ 0 1 0 0 1 0/ 0 0 1 0 0 1]
O2	(oI)	[1 0 0 0 1 0/ 0 1 0 1 0 0/ 0 0 0 0 0 0/ 0 1 0 1 0 0/ 1 0 0 0 1 0/ 0 0 0 0 0 1]
O3	(oI)	[1 0 0 1 0 0/ 0 1 0 0 1 0/ 0 0 0 0 0 0/ 1 0 0 1 0 0/ 0 1 0 0 1 0/ 0 0 0 0 0 0]
O4	(oS)	[0 0 0 0 0 0/ 0 0 0 0 0 0/ 0 0 1 0 0 0/ 0 0 0 1 1 0/ 0 0 0 1 1 0/ 0 0 0 0 0 1]
O5	(oP)	[0 0 0 0 0 0/ 0 0 0 0 0 0/ 0 0 0 0 0 0/ 0 0 0 1 0 0/ 0 0 0 0 1 0/ 0 0 0 0 0 1]
M1A	(mC)	[1 1 0 0 0 0/ 1 1 0 0 0 0/ 0 0 1 0 0 0/ 0 0 0 1 1 0/ 0 0 0 1 1 0/ 0 0 0 0 0 1]
M1B	(mC)	[1 0 0 1 0 0/ 0 1 0 0 1 0/ 0 0 1 0 0 0/ 1 0 0 1 0 0/ 0 1 0 0 1 0/ 0 0 0 0 0 1]
M2A	(mC)	[1 0 0 1 0 0/ 0 1 0 0 1 0/ 0 0 0 0 0 0/ 1 0 0 1 0 0/ 0 1 0 0 1 0/ 0 0 0 0 0 1]
M2B	(mC)	[1 0 0 0 0 0/ 0 1 0 1 0 0/ 0 0 0 0 0 0/ 0 1 0 1 0 0/ 0 0 0 0 1 0/ 0 0 0 0 0 1]
M3	(mC)	[1 0 0 0 0 0/ 0 1 0 0 1 0/ 0 0 0 0 0 0/ 0 0 0 1 0 0/ 0 1 0 0 1 0/ 0 0 0 0 0 0]
M4	(mP)	[0 0 0 0 0 0/ 0 0 0 0 0 0/ 0 0 1 0 0 0/ 0 0 0 1 0 0/ 0 0 0 0 1 0/ 0 0 0 0 0 1]
A1	(aP)	[1 0 0 0 0 0/ 0 1 0 0 0 0/ 0 0 1 0 0 0/ 0 0 0 1 0 0/ 0 0 0 0 1 0/ 0 0 0 0 0 1]
A2	(aP)	[1 0 0 0 0 0/ 0 1 0 0 0 0/ 0 0 0 0 0 0/ 0 0 0 1 0 0/ 0 0 0 0 1 0/ 0 0 0 0 0 1]
A3	(aP)	[1 0 0 0 0 0/ 0 1 0 0 0 0/ 0 0 0 0 0 0/ 0 0 0 1 0 0/ 0 0 0 0 1 0/ 0 0 0 0 0 0]
H4	(hP)	[0 0 0 0 0 0/ 0 0 0 0 0 0/ 0 0 1 1 1 0/ 0 0 1 1 1 0/ 0 0 1 1 1 0/ 0 0 0 0 0 1]

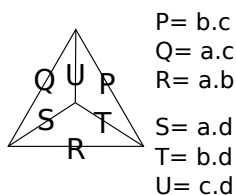


Fig. 1. Bravais triangle with labeling as used in the International Tables

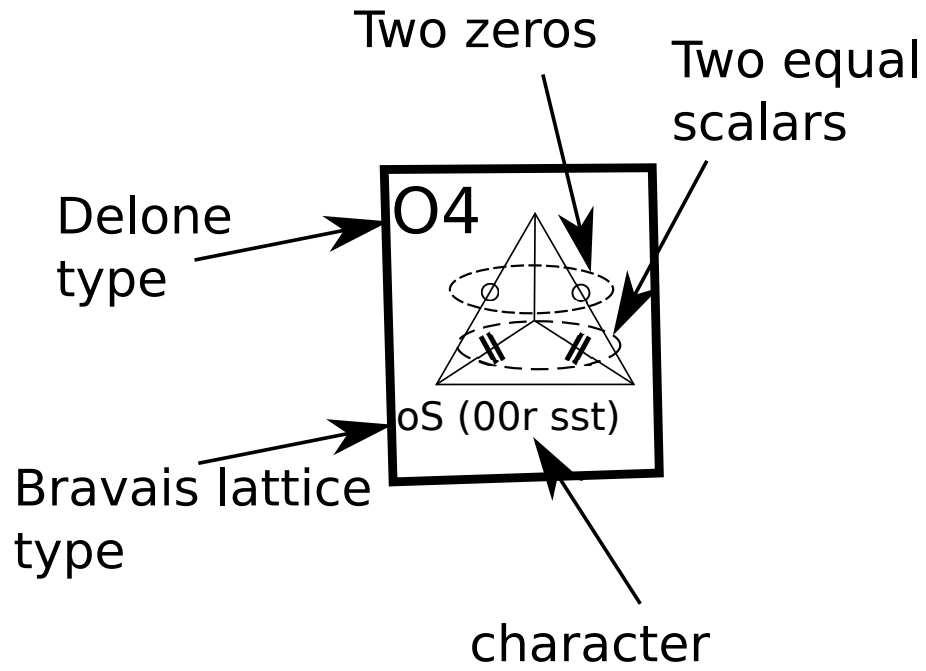
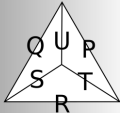
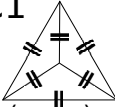
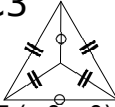
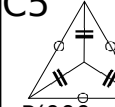
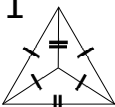
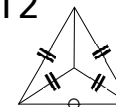
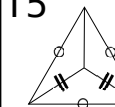
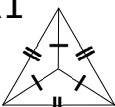
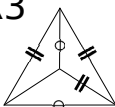

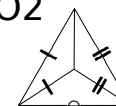
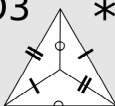
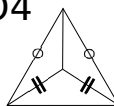
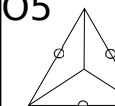
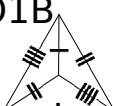
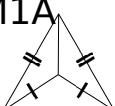
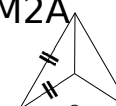
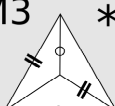

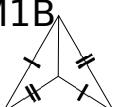

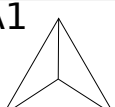
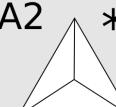
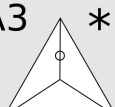
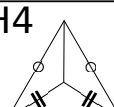


Fig. 2. Delone type description

	1	2	3	4	5
C	C1  cl (rrr rrr)		C3  cF (rr0 rr0)		C5  cP(000 rrr)
T	T1  tl (rrs rrs)	T2  tl (rr0 rrs)			T5  tP(000 rrs)
R	R1  hR (rrr sss)		R3  hR (rr0 sr0)		
O	O1A  oF (rrs rrt)	O2  ol (rs0 srt)	O3 *  ol (rs0 rs0)	O4  oS (00r sst)	O5  oP (000 rst)
O	O1B  ol (rst rst)				
M	M1A  mC (rrs ttu)	M2A  mC (rs0 stv)	M3 *  mC (rs0 ts0)	M4  mP (00r stv)	
M	M1B  mC (rst rsu)	M2B *  mC (rs0 rst)			
A	A1  aP (rst uvw)	A2 *  aP (rs0 tuv)	A3 *  aP (rs0 tu0)		
H				H4  hP (00r rrs)	

* The right angles have no relationship to symmetry.

Fig. 3. The Delone types

Nullspace dimension	Free parameters							
5	1	C1 cl (rrr rrr)	C3 cF (rr0 rr0)	C5 cP(000 rrr)				
4	2	T1 tl (rrs rrs)	T2 tl (rr0 rrs)	T5 tP(000 rrs)	R1 hR (rrr sss)	R3 hR (rr0 sr0)	O3 ol (rs0 rs0)	H4 hP (00r rrs)
3	3	O1A oF (rrs rrt)	O2 ol (rs0 srt)	O4 oS (00r sst)	O5 oP (000 rst)	O1B ol (rst rst)	M3 mC (rs0 ts0)	M2B mC (rs0 rst)
2	4	M1A mC (rrs ttu)	M1B mC (rst rsu)	M2A mC (rs0 stv)	M4 mP (00r stv)	A3 aP (rs0 tu0)		
1	5	A2 aP (rs0 tuv)						
0	6	A1 aP (rst uvw)						

Fig. 4.

The red points indicate the original circle. The blue points are for the reduced cells.

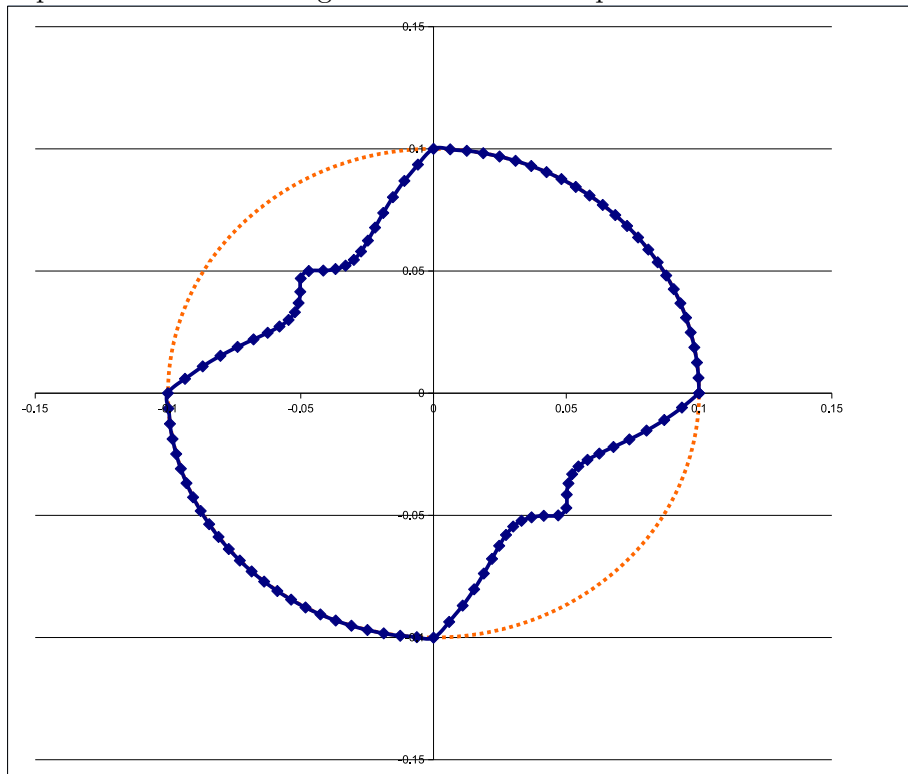


Fig. 5. Delone type M4: there are two zeros. A circle of 100 points with radius 0.1 is centered at 0,0. The lattices are reduced and the points are plotted at the distance from M4.

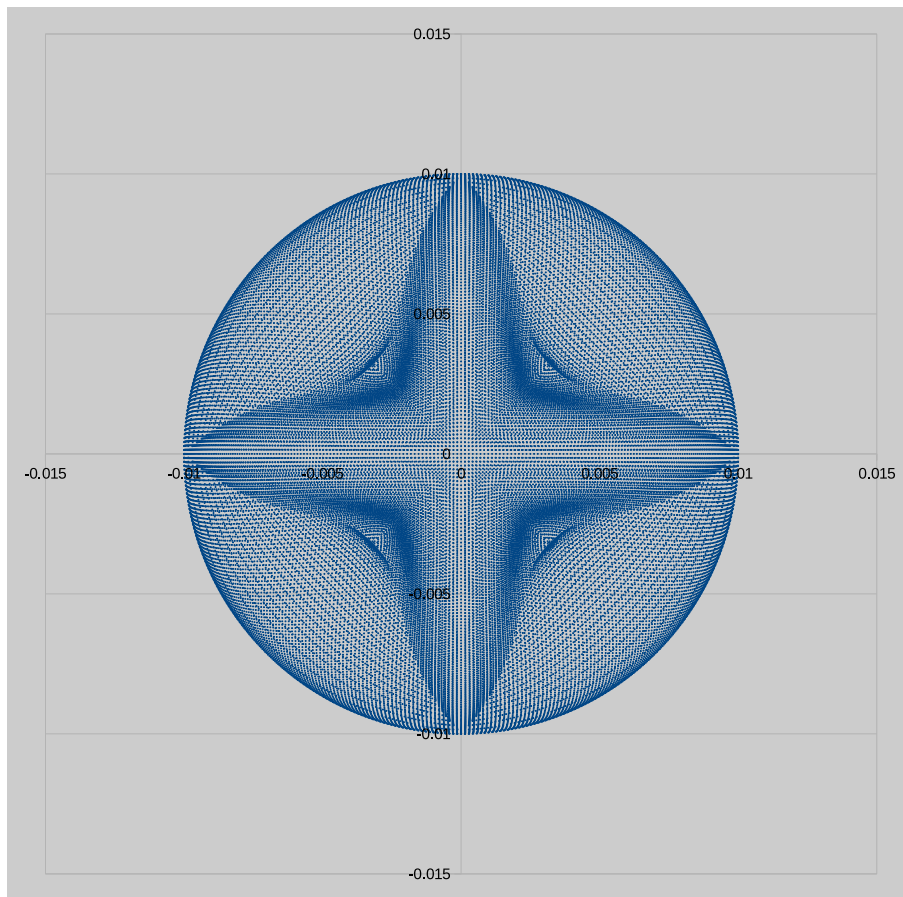


Fig. 6. Delone type O5: there are three zeros. A sphere is centered at 0,0,0, with radius 0.1. The lattices are reduced, and the point is placed at a distance equal to the distance from type O5. 50,000 points are plotted.

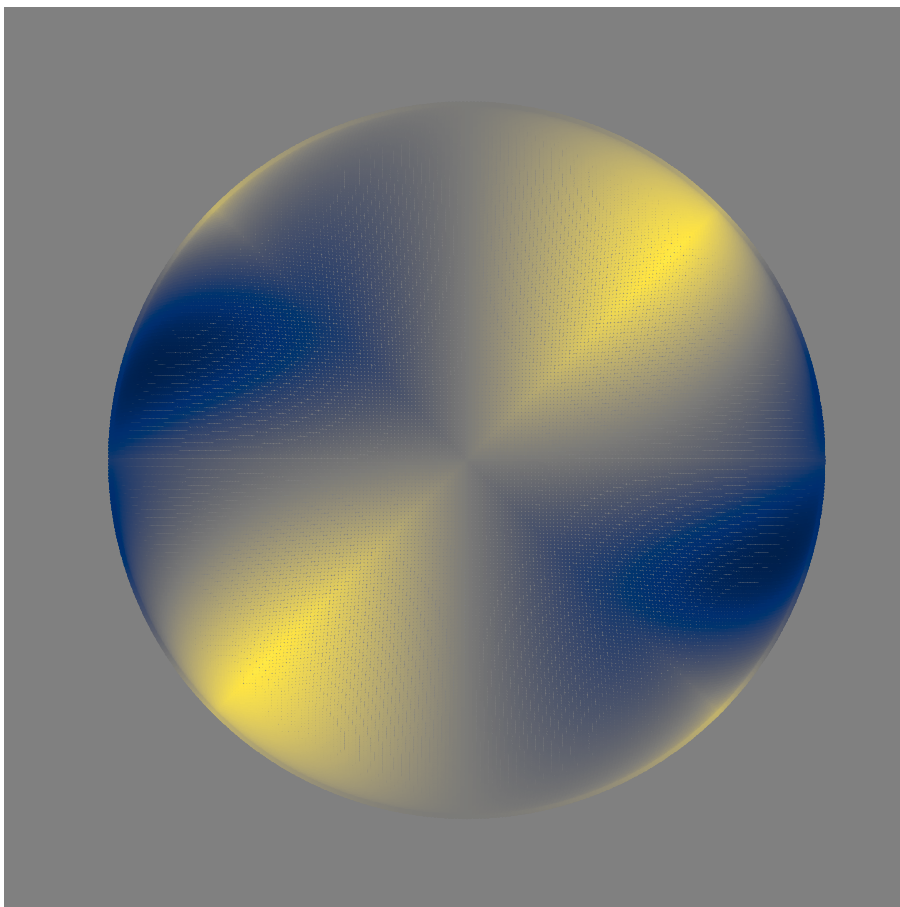


Fig. 7. Delone type O4: There are two zeros and one pair. A sphere with radius 0.1 was placed around one point. At each sphere point, the lattice was reduced and the point on the sphere was assigned a color (0.01) to blue (0.0075). 100,000 points are plotted.

Synopsis

A method for determining likely Bravais lattice types based on Selling (Delone) reduction. It is a complete, closed solution.
